PP-AWARE: Task 3.5 - LPI verification and correlation of convective events with microphysical and thermodynamical indices

F. Gofa, D. Boucouvala, HNMS

1. Approach

The distribution analysis of several convective events in both space and time will allow lightning/thunderstorm regimes to be determined. Lightning Potential Index (LPI) is a measure of the potential for charge generation and separation that leads to lightning flashes in convective thunderstorms and can be calculated from COSMO model. While the connection between cloud microphysics and lightning seems apparent, the common indices used for forecasting thunderstorms and the potential for lightning usually rely on stability and thermodynamical indices (e.g., CAPE).

An effort will be given to correlate LPI with observed lightning. In this way, it will be evaluated if for Greek territory LPI can be useful parameter for predicting lightning as well as a tool for improving weather forecasting of convective storms and heavy rainfall. Statistical evaluation of LPI forecasts with traditional dichotomic scores as well as with SAL spatial method on selected intense convective events will be also performed by comparing gridded lightning data with model forecasts. LPI will be evaluated (optimum upscale window) over Greece on certain events, as a useful parameter for predicting lightning as well as a tool for improving weather forecasting of convective storms and heavy rainfall.

2. Lightning formation

The microphysical processes that lead to the formation of precipitation particles are involved in charge separation and the buildup of electric fields in convective clouds.

The noninductive mechanism, involves rebounding collisions between graupel particles and cloud ice crystals and requires the presence of supercooled liquid water. Lightning Potential Index (LPI) is a measure of the potential charge separation that leads to lightning flashes in convective thunderstorms (Yair et al. 2010, JGR). It is calculated from model simulated updraft and microphysical fields within the charge separation region of clouds between (0° C and $- 20^{\circ}$ C), where the non-inductive mechanism involving collisions of ice and graupel particles in the presence of supercooled water is most effective (Saunders, 2008).

LPI is defined as the volume integral of the total mass flux of ice and liquid water within the "charging zone" in a developing thundercloud. The LPI (J kg-1) and is defined as:

$$LPI = \frac{1}{V} \iiint \in \omega^2 dxdydz \qquad \in = 2\left(Q_i Q_l\right)^{0.5} / \left(Q_i + Q_l\right)$$

Where V is the volume of air in the layer between 0°C and -20°C, w is the vertical wind component (ms-1) and qs, qi and qg are the model-computed mass mixing ratios for snow, cloud ice, and graupel respectively (in kg-1). € is a dimensionless number that has a value between 0 and 1 and is defined by the formula above.

Where: Q_l is the total liquid water mass mixing ratio and Q_i is the ice fractional mixing ratio (kg kg-1) defined by,

$$Q_i = q_g \left[\left(\left(q_s q_g \right)^{0.5} / \left(q_s + q_g \right) \right) + \left(\left(q_i q_g \right)^{0.5} / \left(q_i + q_g \right) \right) \right]$$

ε is a scaling factor for the cloud updraft and attains a maximal value when the mixing ratios of supercooled liquid water and of the combined ice species (the total of cloud ice, graupel, and snow) are equal.

Calculation of the LPI from the cloud-resolving atmospheric model output fields can provide maps of the microphysics-based potential for electrical activity and lightning flashes.

3. Methodology

Model setup: LPI can only be calculated if you run model with the graupel microphysics (itype_gscp=4) or the 2-moment microphysics. Results for LPI are only meaningful in convection resolving mode, i.e., deep convection parameterization switched off and grid spacing smaller or equal to 4 km. LPI is a column integral involving the square of the vertical velocity and the presence of graupel (=riming process) and other ice hydrometeors at the same locations. It needs explicitly simulated convective cells with realistic updraft speeds.

The COSMO-GR4 LPI forecasts were used with 0.04 deg resolution forecasts (not a operational product) as well as CAPECON outputs, while other indices were calculated from model outputs. This serves as the original resolution of the analysis performed. Then aggregated forecast and observations gridded format with multiple of the original space resolution are calculated through scripts that were developed.

Forecasts gridded fields: For the original resolution (0.04), the LPI value of each grid point is checked, and if it is higher than the value of 0.3 (see table below) , a value of 1 is given to the specific grid point. Next, grids with increased (multiple) resolution based on the original dimensions are created (e.g., 0.04x2, 3, …, 20). For each new grid cell or each new grid, the MAX LPI value of the 3x3 points is assigned.

LPI_MAX$_{3x3}$ = LPI_MAX in einer 3x3 GP Umgebung

o Mai – August: LPI_MAX$_{3x3}$ > 10^{-3} J/kg und RG ≥ 0.0 mm/h
o März, April, September: LPI_MAX$_{3x3}$ > 0.2 J/kg und RG ≥ 1.2 mm/h
o Oktober – Februar: LPI_MAX$_{3x3}$ > 0.5 J/kg und RG ≥ 3.0 mm/h

Observations: For all new grids with resolution from 0.04deg up to 20x0.04deg, a lat-lon based check is performed in the boundaries of each grid cell, for the existence of lightning observations and a value of 1 is assigned to that grid point for positives checks or else a value of zero.

Statistics:
To statistically evaluate LPI forecast performance the following are applied:
➢ Direct comparison of obs-fcs gridded values and calculation of contingency table properties.
➢ SAL methodology for steady LPI threshold of one (lightning existence).

4. Theromodynamical indices

Stability indices were calculated using temperature and relative humidity profiles from the COSMO-GR4 model forecasts. The formulas used for the estimation of the various indices in this analysis are specified below.

a. K index (KI)

It calculates the thunderstorm potential based on the vertical temperature lapse rate between 850 and 500 mbar pressure levels, moisture content at 850 mbar pressure and moist layer depth at 700 mbar pressure (George 1960).

$$KI = (T_{850}-T_{500})+Td_{850}-(T_{700}-T_{700}),$$

with the suffix values indicating the pressure level.

The critical values of KI index indicating thunderstorm activity (Johnson 1982) are given below:

KI (K)	THUNDERSTORM CHANCES
UNDER 288	0% Chance
IN THE MIDDLE OF 288 AND 293	20% chance
IN THE MIDDLE OF 294 AND 298	20-40% possibility for little thunderstorms
IN THE MIDDLE OF 299 AND 303	40-60% possibility for little to medium thunderstorms
IN THE MIDDLE OF 304 AND 308	60-80% possibility for heavy thunderstorms
IN THE MIDDLE OF 309 AND 313	80-90% possibility for severe thunderstorm event
ABOVE 313	Over 90% possibility for thunderstorm event

b. Total Totals Index (TTI)

The TTI is procured by basic deduction among temperature and dew point temperature values at 850 and 500 hpa pressure levels (Miller 1967).

Cross totals, $CT = Td_{850} - aT_{500}$; Vertical totals, $VT = T_{850} - T_{500}$

$$\text{Total Totals Index, } TTI = CT + VT = T_{850} + Td_{850} - 2T_{500}$$

The critical threshold values of TTI parameter (Miller 1972) are given below:

ITTI VALUES (K)	THUNDERSTORM POSSIBILITY
RANGING BETWEEN 44 AND 45	Possibility for small thunderstorm activity
RANGING BETWEEN 46 AND 47	Possibility for moderate thunderstorm activity
RANGING BETWEEN 48 AND 49	Possibility for moderate to severe range of thunderstorm activity
RANGING BETWEEN 50 AND 51	Possibility for heavy thunderstorm activity
RANGING BETWEEN 52 AND 55	Possibility for scattered thunderstorm activity
ABOVE 55	Possibility for severe thunderstorm activity

c. Improved total totals index

The improved total totals index is obtained by the average of the temperatures at surface (at 2 m), the 925hpa and the 850hpa pressure levels (Miller 1967).

$$ITTI = (2mT+ Td_{925}+T_{850})/3 +(2mTd+ Td_{925}+Td_{850})/3 - 2T_{500}$$

The threshold for thunderstorm occurrence is usually seen at 57 K.

d. Humidity Index (HI)

It is obtained by calculating the availability of water vapour at 850, 700 and 500 hPa pressure levels. The importance of relative humidity as the major component needed for the severe thunderstorm activities is being estimated by this index.

$$HI= (T_{850}-Td_{850})+(T_{700}-Td_{700})+(T_{500}-Ts_{500})$$

When HI values lies less than or equal to 30K, high possibility for thunderstorm occurrence has been noticed on that region.

e. Convective available potential energy (CAPE)

The buoyant energy required to accelerate an air parcel vertically is referred to as CAPE. The sum of positive buoyant energy from the level of free convection to the equilibrium level can be used to measure it (Moncrieff and Miller 1976).

$$CAPE = \int_{x}^{y} g\left[\frac{TV_{parcel} - TV_{env}}{TV_{env}}\right] dz$$

Where TV_{parcel} represents the parcel's virtual temperature and TV_{env} represents the virtual temperature of environment respectively. x and y denote the level of free convection and neutral buoyancy.

The critical values of cape parameter (Grieser 2012) are:

CAPE (IN J/KG)	Thunderstorm chances
UNDER 300	no energy for convection
FROM 300 TO 1000	Poor potential for weak convection
FROM1000 TO 2500	moderate potential for convection
GREATER THAN 2500	strong potential for convection

5. Selection of intense precipitation events

For the application of the methodology, eight test cases with significant convective precipitation amounts around Greece were analyzed, thus only three of them were proved to be significant and presented with respect to the LPI values forecasted.

    I. Test Case 1: 15 Nov 2017
    II. Test Case 2: 12 Nov 2019
    III. Test Case 3: 24 Nov 2019

Other cases analyzed were: 10/07/2019, 07/12/2020, 08/08/2020, 02/06/2018, 03/10/2019. Below the synoptic description for weather situation is provided.
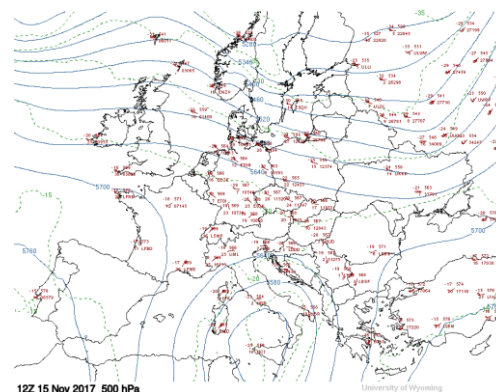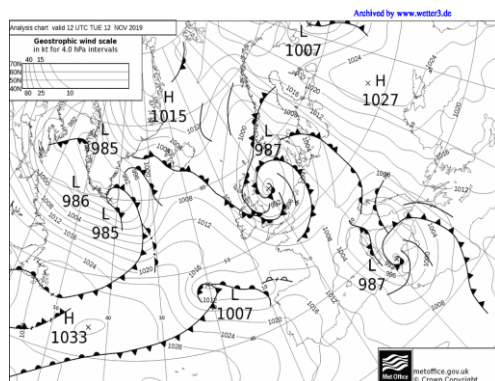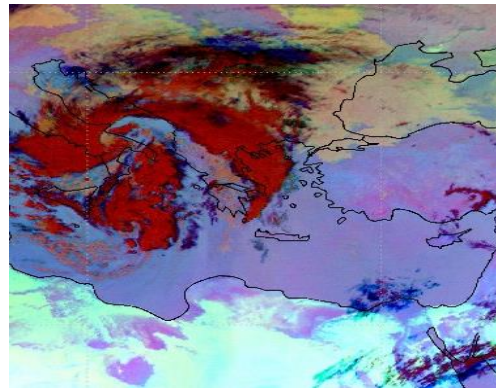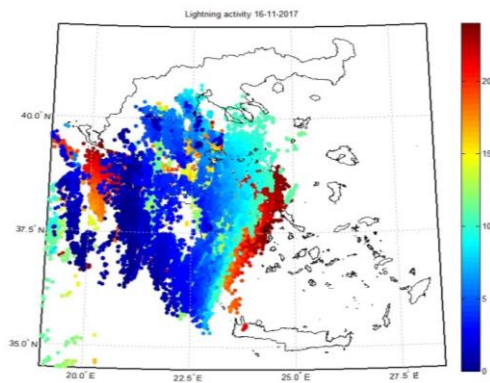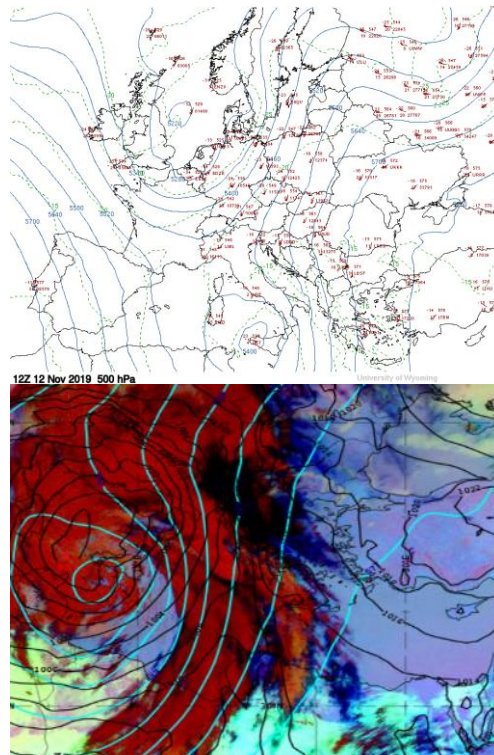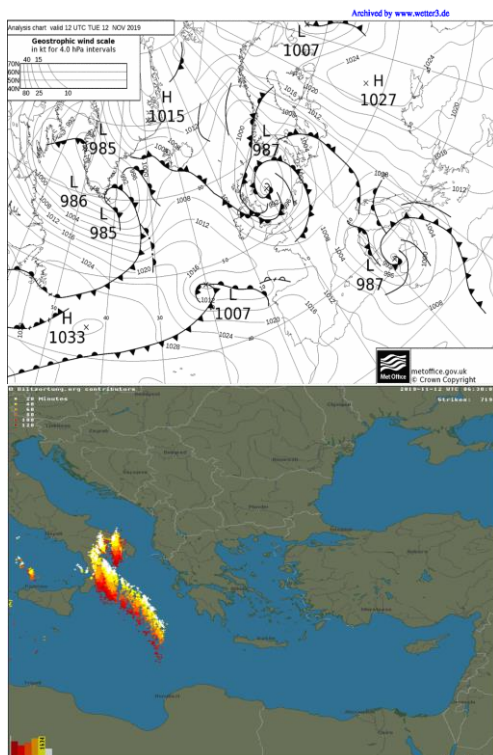
Figure 1: Upper row: MSLP maps during the event. Lower row:.Accumulated observed lightnings (left) and RBG air masses.

I. Test Case 1

A cut-off low in Tunisia over upper troposphere on 11/11/2017 associated with a low over Syrti Gulf which caused severe thunderstorms over Central Mediterranean, moved northeastwards and on 13/11 influenced initially western Greece and gradually east parts, mainly Attica, Cyclades, Crete and Dodecanese with heavy phenomena. In addition, on 13/11 a second deep low over Genoa Gulf (995hpa) transferred polar air masses over Southern Italy. On 15/11 the low expanded and moved over Central Mediterranean. Over the warm sea of Ionian, the cold air destabilized. Due to weak wind shear, a cyclone (Medicane) was formed. Heavy rainfall and flooding caused severe damages over Western Attica (Fig. 1).

II. Test Case 2

Deep barometric low with frontal activity over South Italy moved north eastwards leading to strong gale southerly winds (9 Beaufort), heavy rain, thunderstorms and electrical discharge all over Greece (except Dodecanese). Flooding over Attica and Crete were reported while Ionian islands suffered from severe damages especially Corfu and Cefalonia (Fig.2)

.

Figure 2: Upper row: MSLP maps during the event. Lower row:.Accumulated observed lightnings (left) and RBG air masses.


III. Test Case 3

Deep low over Italy moved eastwards and produced a cold front over Ionian Sea which influenced all the country of Greece with severe damages due to heavy rainfall. Floodings were reported in South Attica, Rhodes, Central Macedonia and East Aegean Islands. Strong southerly gale winds 9Bf over all seas. First snowfall of the year was reported in mainland mountains (Fig.3).
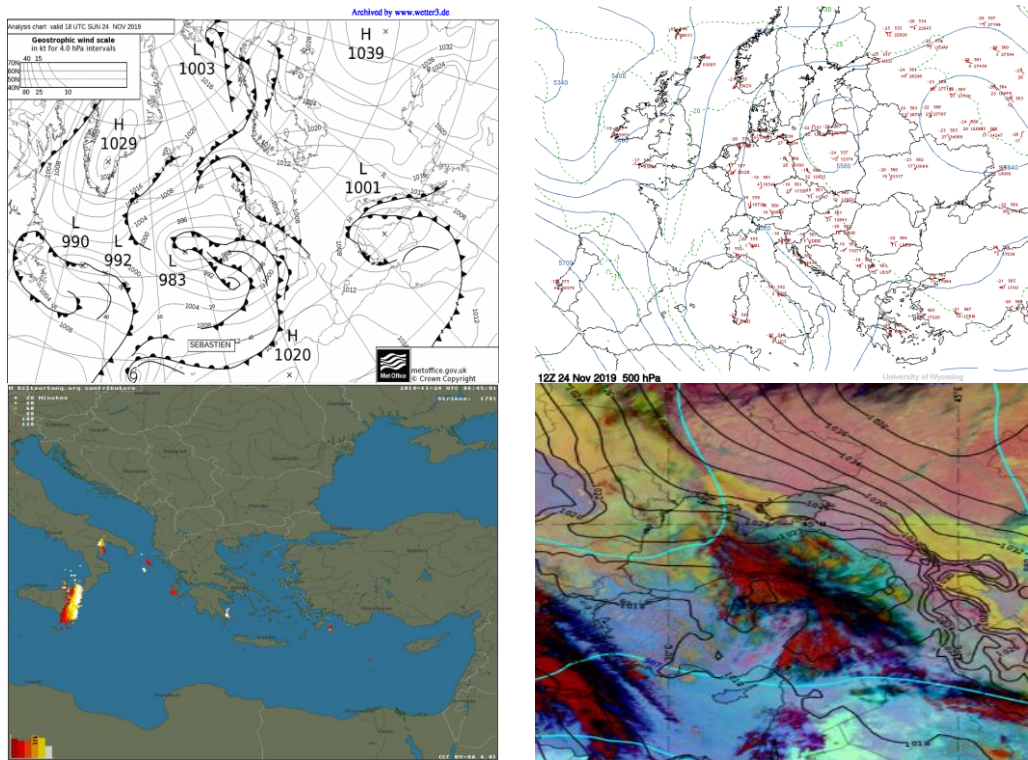
Figure 3: Upper row: MSLP maps during the event. Lower row: accumulated observed lightnings (left) and RBG air masses.

6. Evaluation of LPI Forecasts – Dichotomic Approach

In this section, the statistical results of the evaluation of the upscaled forecast and observation fields are presented. The methodology presented in section 3 was applied for all three test cases and the relevant plots for POD, FAR, ETS and FBI.
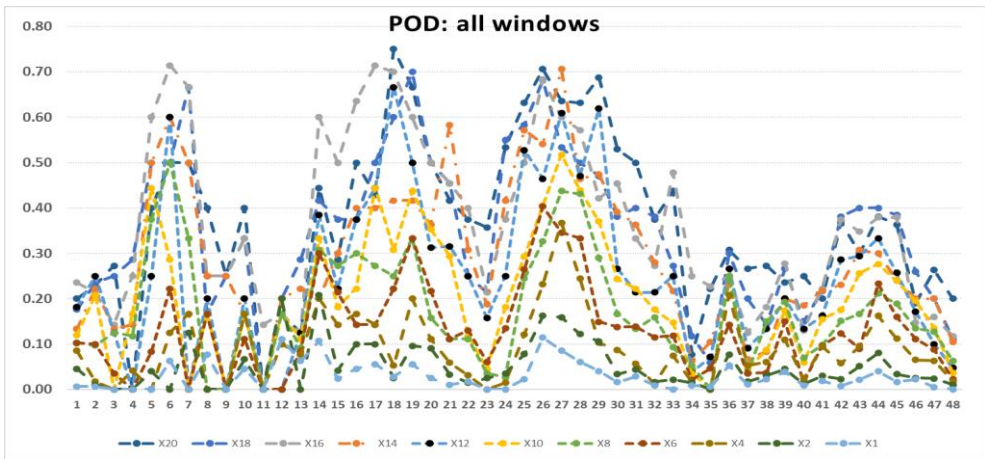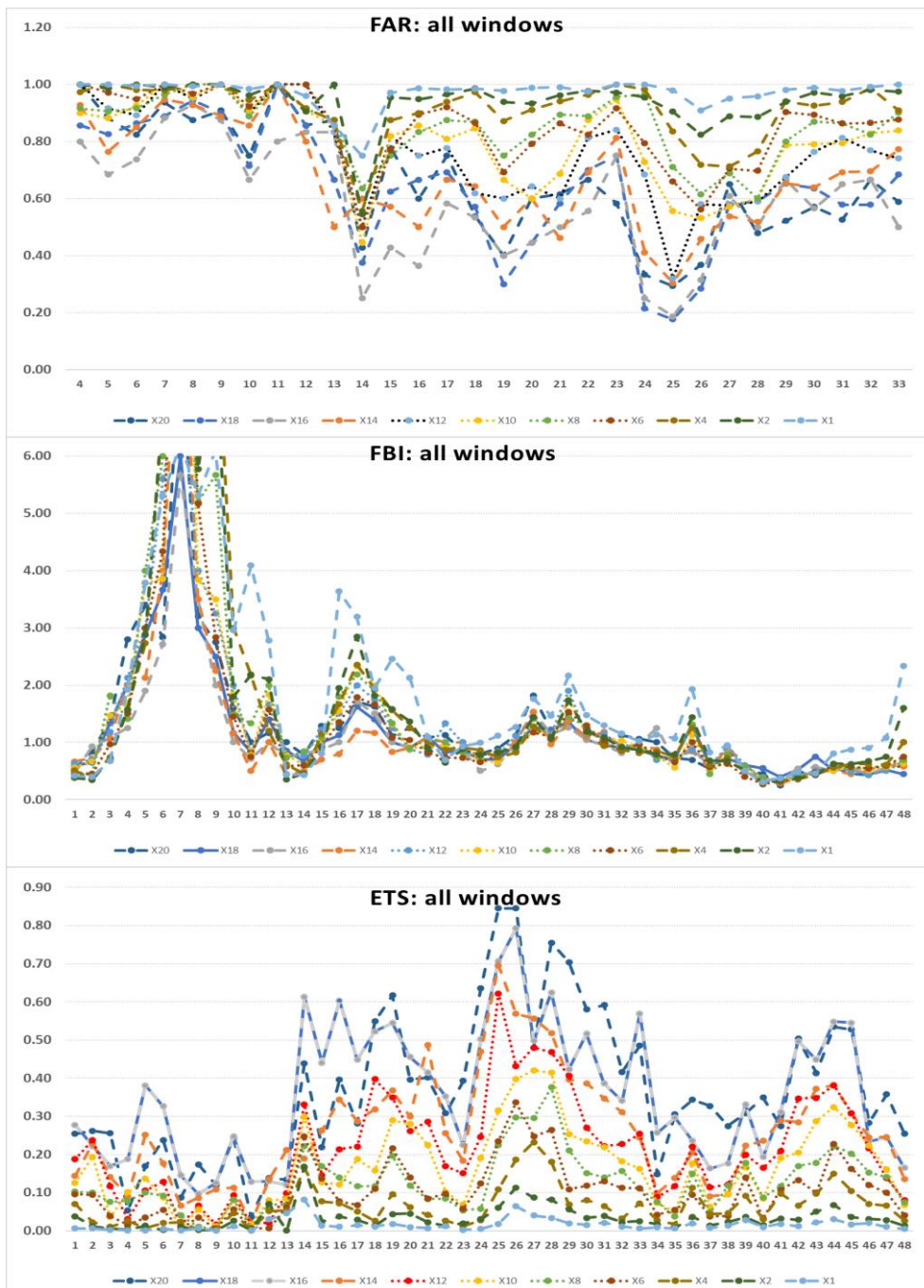
Figure 4: Test case 1 - From top to bottom: POD, FAR, FBI, ETS for various time intervals during the event and for increasing spatial resolution.
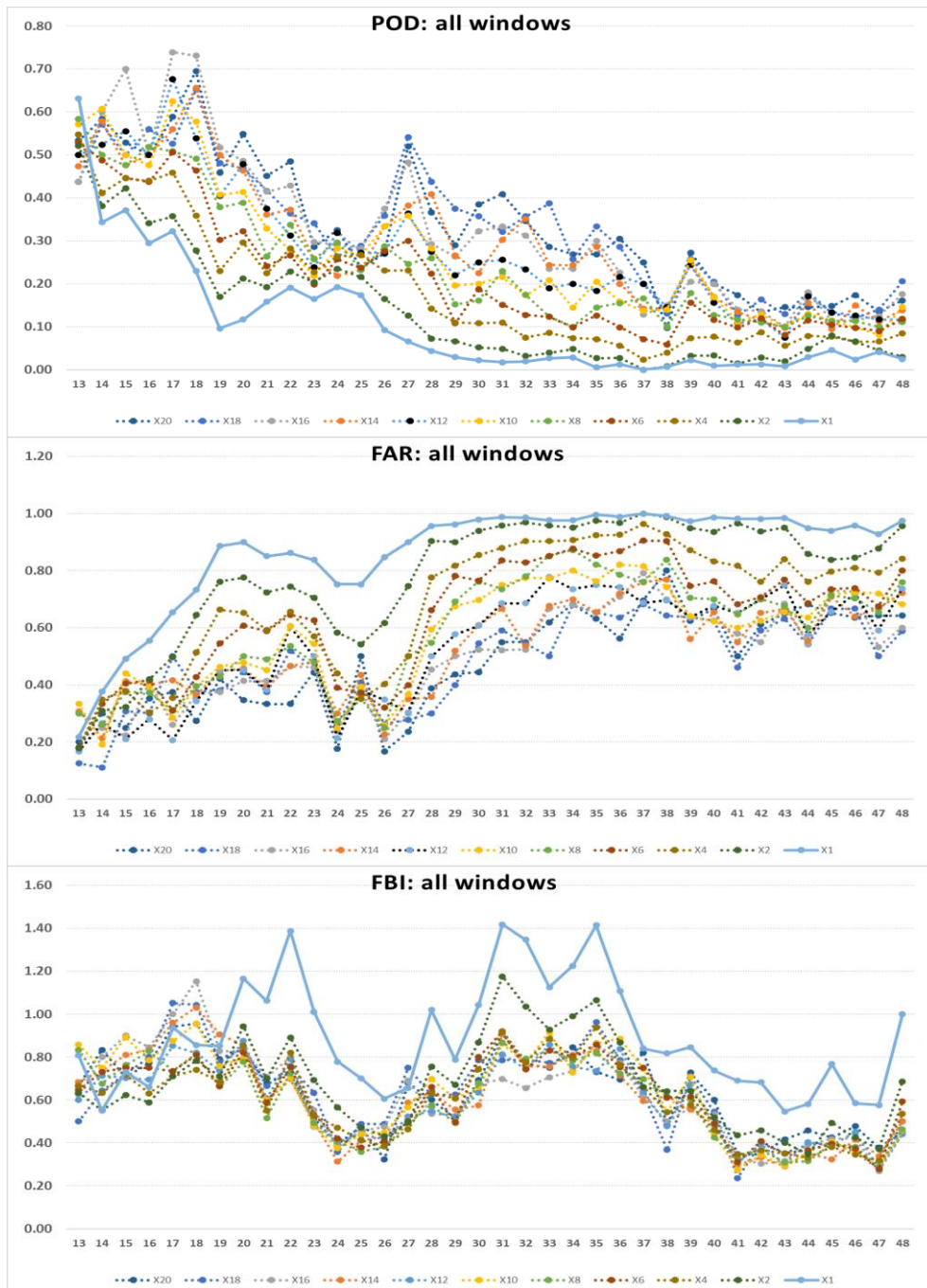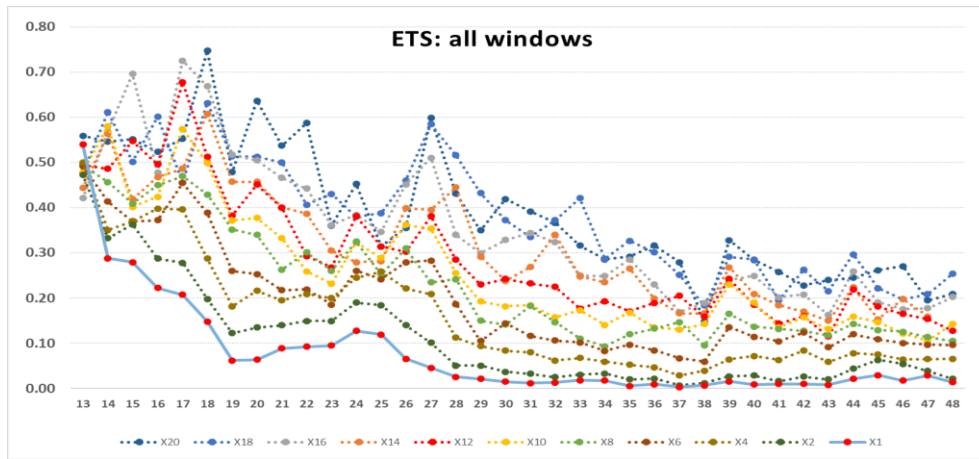
Remarks from Test Case 1: No skill for LPI forecasts for the first 12h of the event
POD: reduced skill during afternoon hours, improved performance for scales larger than 16x0.04~64km
FAR: Improved performance for scales higher than 14x0.04~56km, no variation in performance with lead time.
FBI: no impact of the upscaling approach in the performance, high overestimation in first 10 forecast hours
ETS: performance does not increase linearly with increased resolution, optimum skill in most time intervals when the 64km resolution is applied.
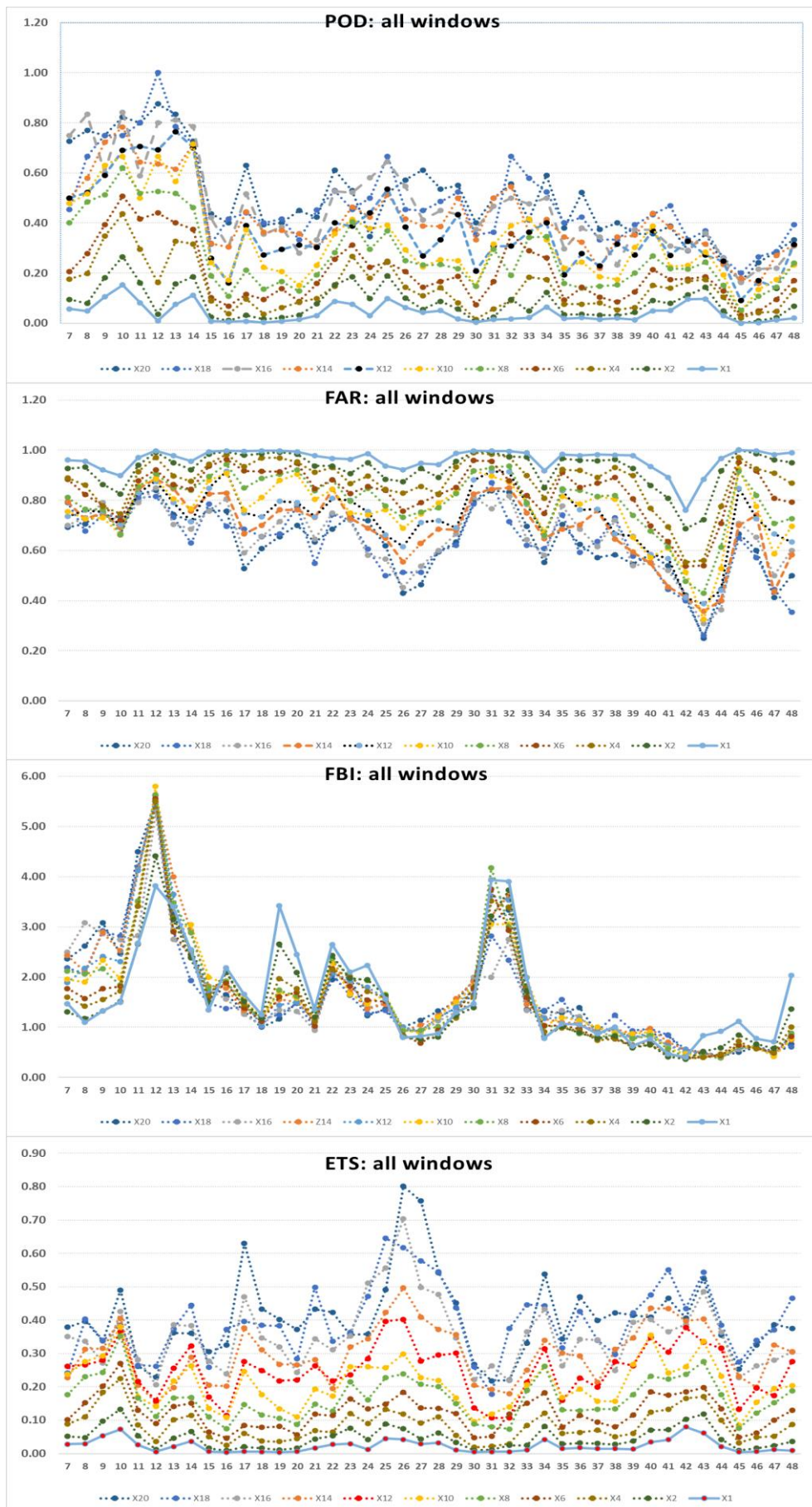
Figure 5: Test case 2 - From top to bottom: POD, FAR, FBI, ETS for various time intervals during the event and for increasing spatial resolution.

Remarks from Test Case 2: No skill of forecasted fields in the original resolution
POD: no change in skill with lead time. Improved performance for scales higher than 12x0.04~48km with no clear improvement in further upscaled fields.
FAR: Improved skill for almost all fields during evening hours
FBI: no impact of the upscaling approach in the performance, higher overestimation for the original resolution but also for almost all upscaled forecasted fields.
ETS: performance increases linearly with window size until 14x0.04deg~56km

Figure 5: Test case 3 - From top to bottom: POD, FAR, FBI, ETS for various time intervals during the event and for increasing spatial resolution.

Remarks from Test Case 3: Good performance of LPI forecasts for this event compared to the previous cases even with the original resolution.
POD: Skill is reduced with lead time
**FAR:** For resolution higher than 10x0.04~40km has reached already adequate skill.
FBI: Small underestimation of LPI predictions is shown in all upscaled grids
ETS: Performance increases linearly with window size. For windows higher than 40km there is a good skill in LPI forecasts.

7. Evaluation of LPI Forecasts – SAL Approach

During the application of Structure, Amplitude, Location (SAL) spatial methodology the original resolution of both forecast and observed fields was used.
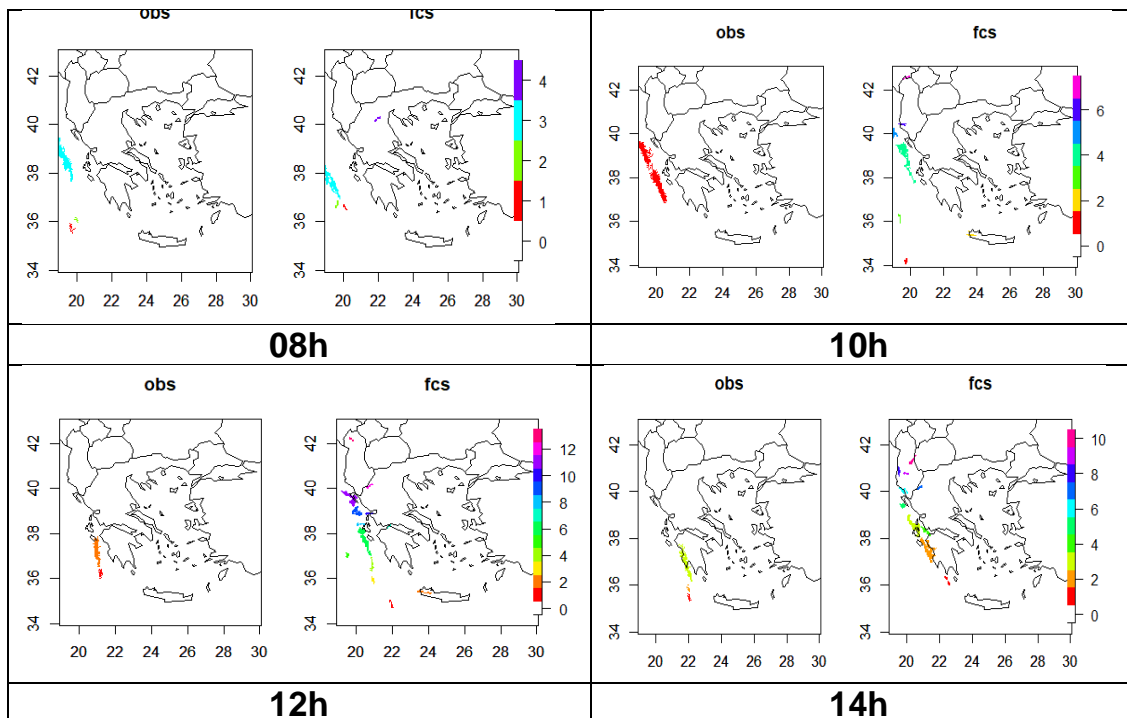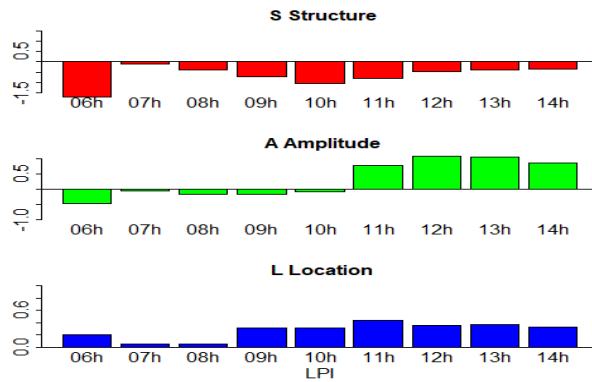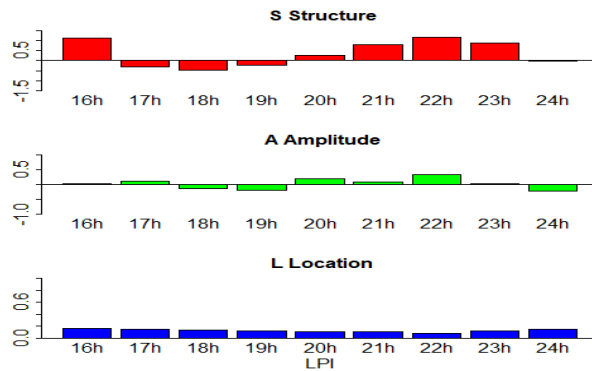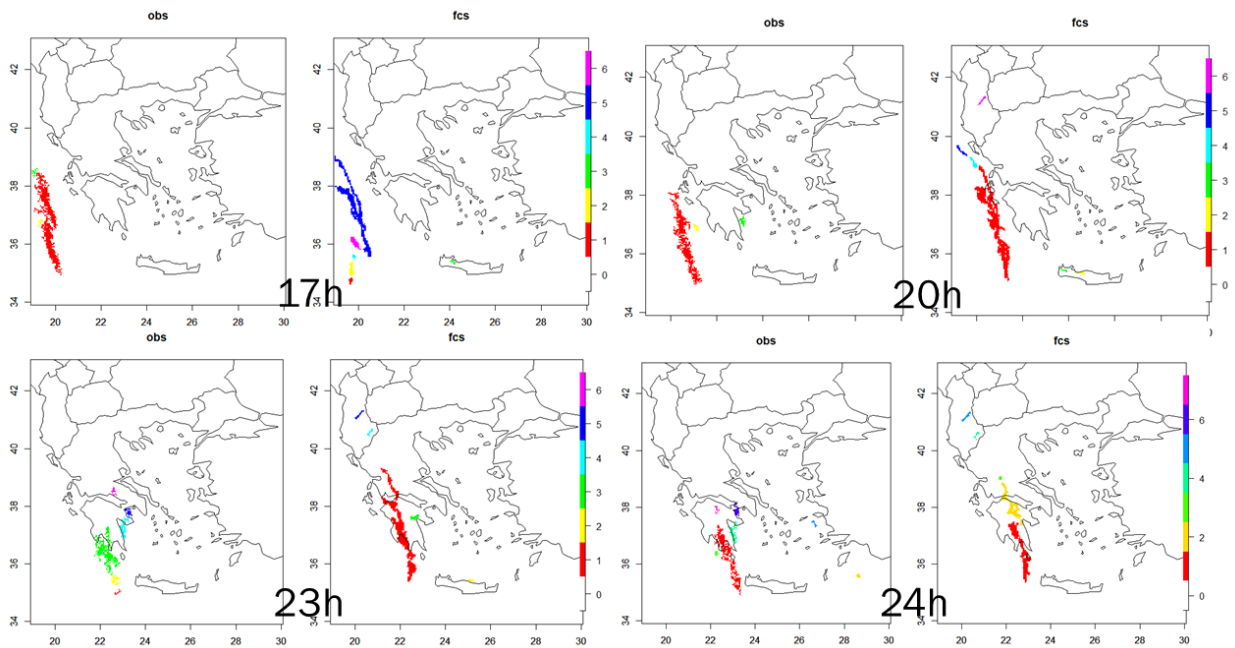
Figure 10: Test case 2 – Objects matching for several time windows during the event. SAL components With respect to forecast horizon.

Remarks from Test Case 2:

The S values are negative, indicating that the model predicts sharper objects than the ones observed.

The A is positive with value higher than 0.5 during afternoon hours (total LPI overestimated as shown in FBI index in upscaling approach).

The L parameter is also increases after 09h, indicating some differences in the location of objects with respect to the observed ones.

Figure 10: Test case 3 – Objects matching for several time windows during the event. SAL components with respect to forecast horizon.

Remarks from Test Case 3:
The S values trend is variable with horizon time and seems that model predicts more widespread objects in the beginning and around the end of the forecasted peried.
The A absolute values are smaller than 0.5 while the total LPI is satisfactorily predicted (slightly overforecasted mainly around 20-23h).
The L parameter is low (around 0.2) and shows good agreement on the location of objects with respect to the observed ones.

8. Post Precessed Thermodynamical Indices

Using the necessary forecasted fields in the original resolution, several thermodynamical indices were calculated and plotted according to the information provided in paragraph 4. Appropriate color pallets were utilized for each index in order to notify areas with high possibility of presence of convection.
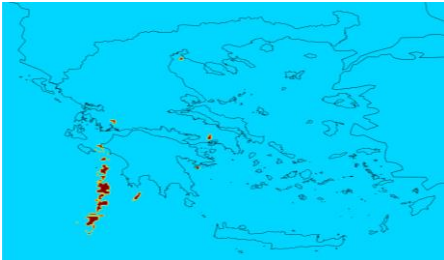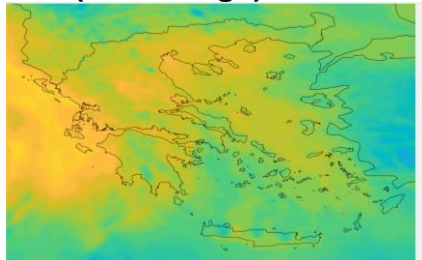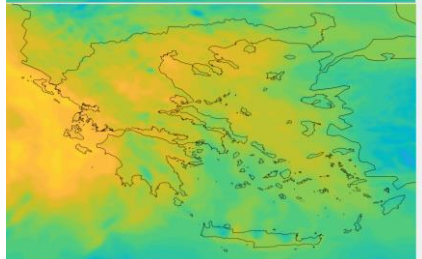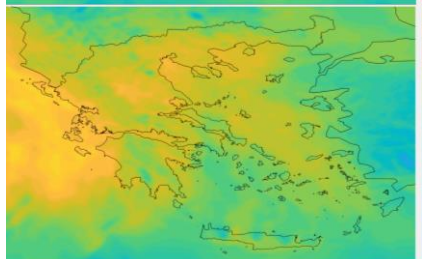
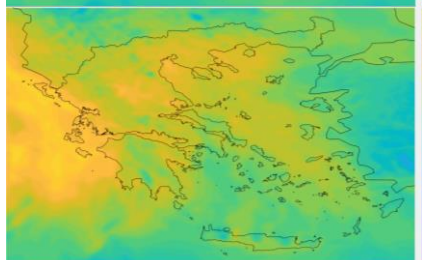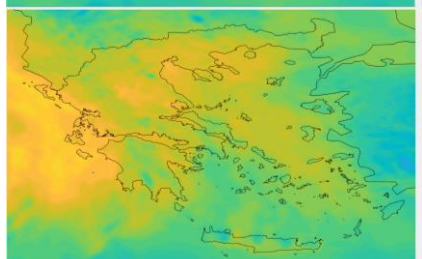| hr	KI (>305 orange)	HI (<30 bluegreen)	CAPE (>1300 bluegreen)
3			
4			
5			
6			
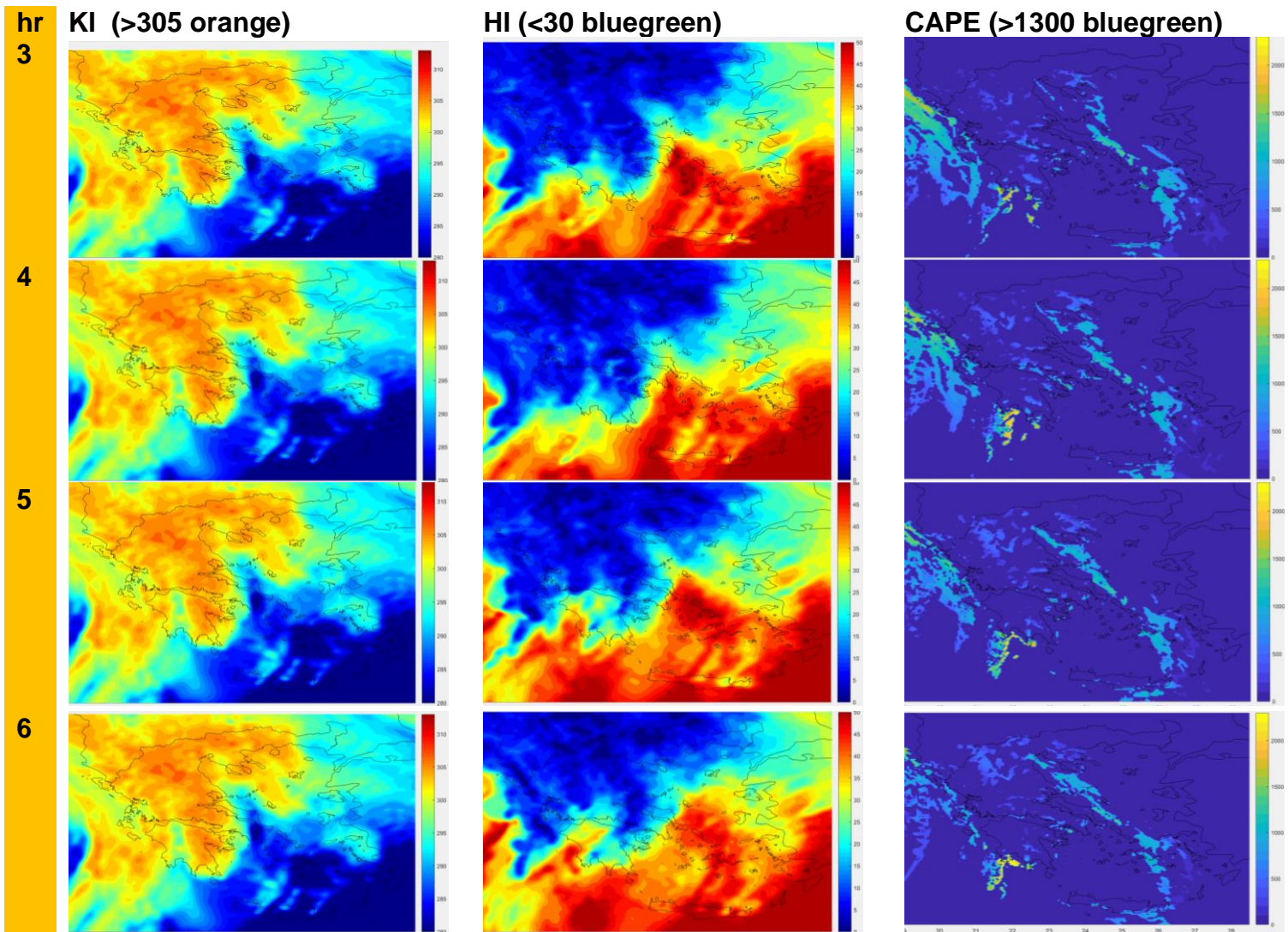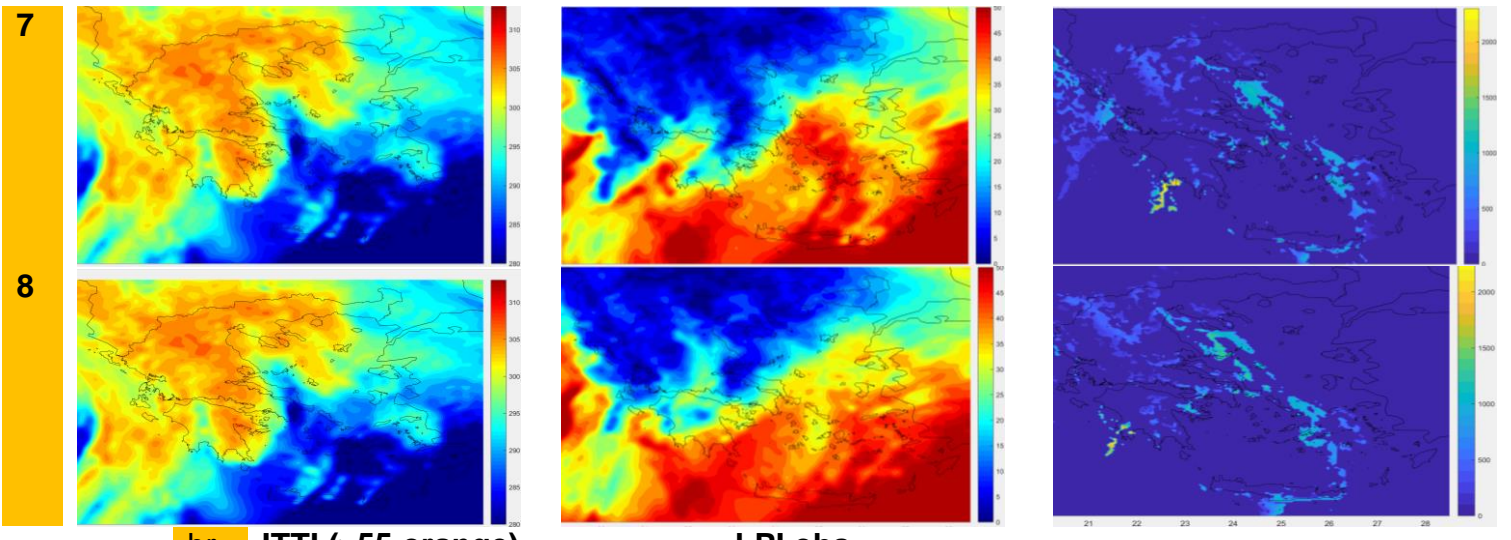
| | ITTI (>55 orange) | LPI obs |

Figure 11: Test case 1 – Presentation of various thermodynamical indices during the evolution of the event with indication of color/threshold that corresponds to high convection probability.

hr	KI (>305 orange)	HI (<30 bluegreen)	CAPE (>1300 bluegreen)
16			
17			
18			
19			
20			

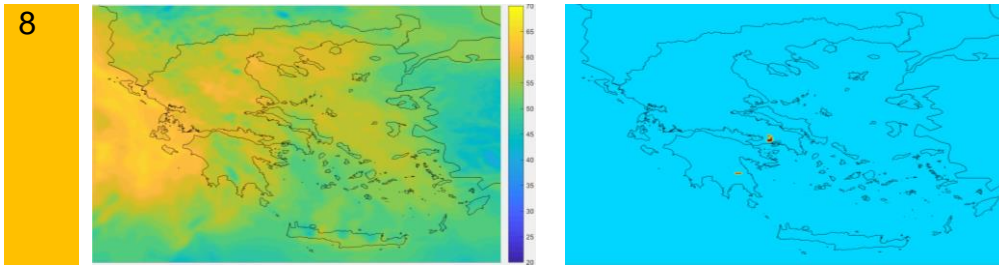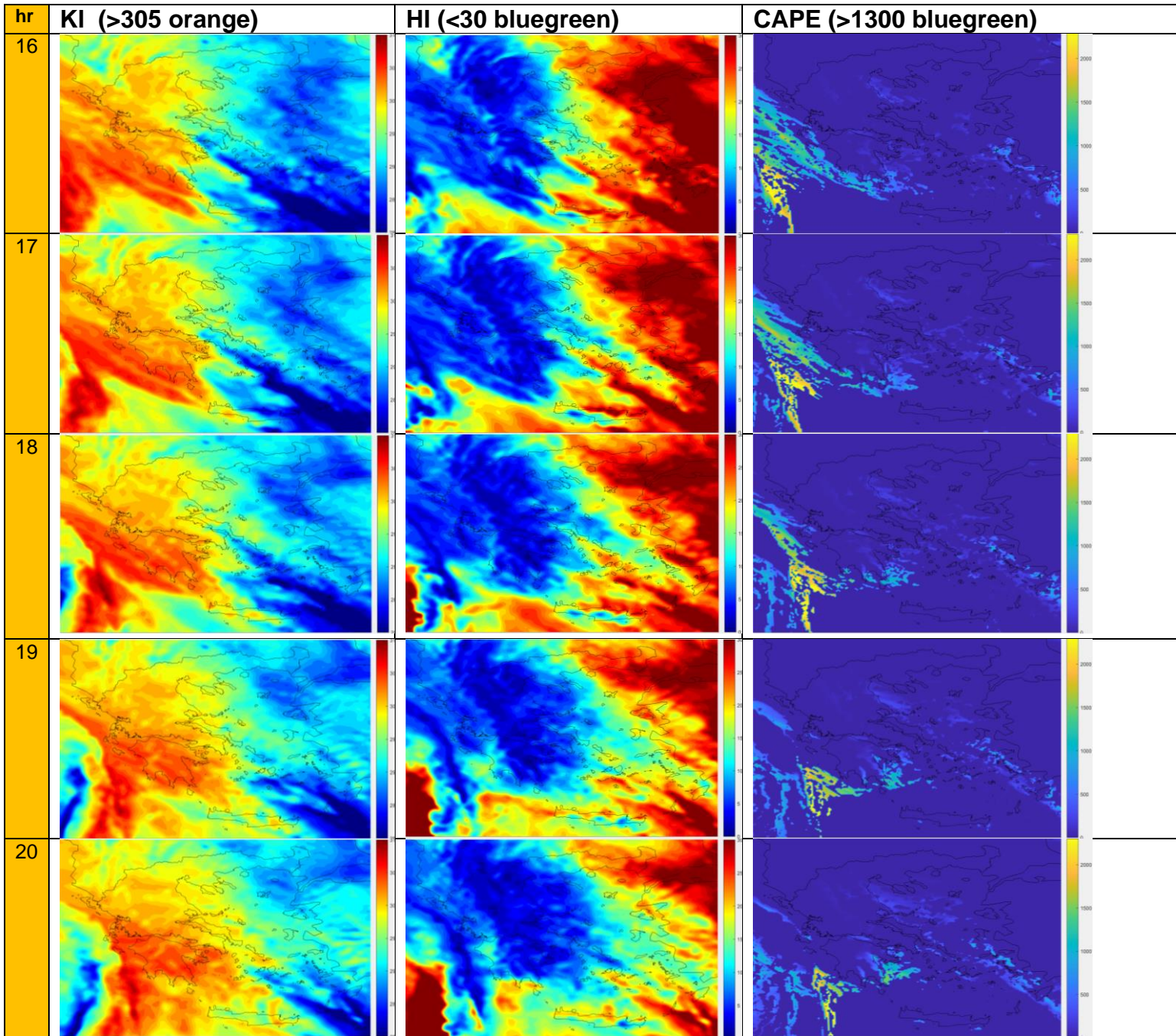| hr	ITTI (>55 orange)	LPI obs
16		
17		
18		
19		
20		
21		

Figure 12: Test case 2 – Presentation of various thermodynamical indices during the evolution

of the event with indication of color/threshold that corresponds to high convection probability.
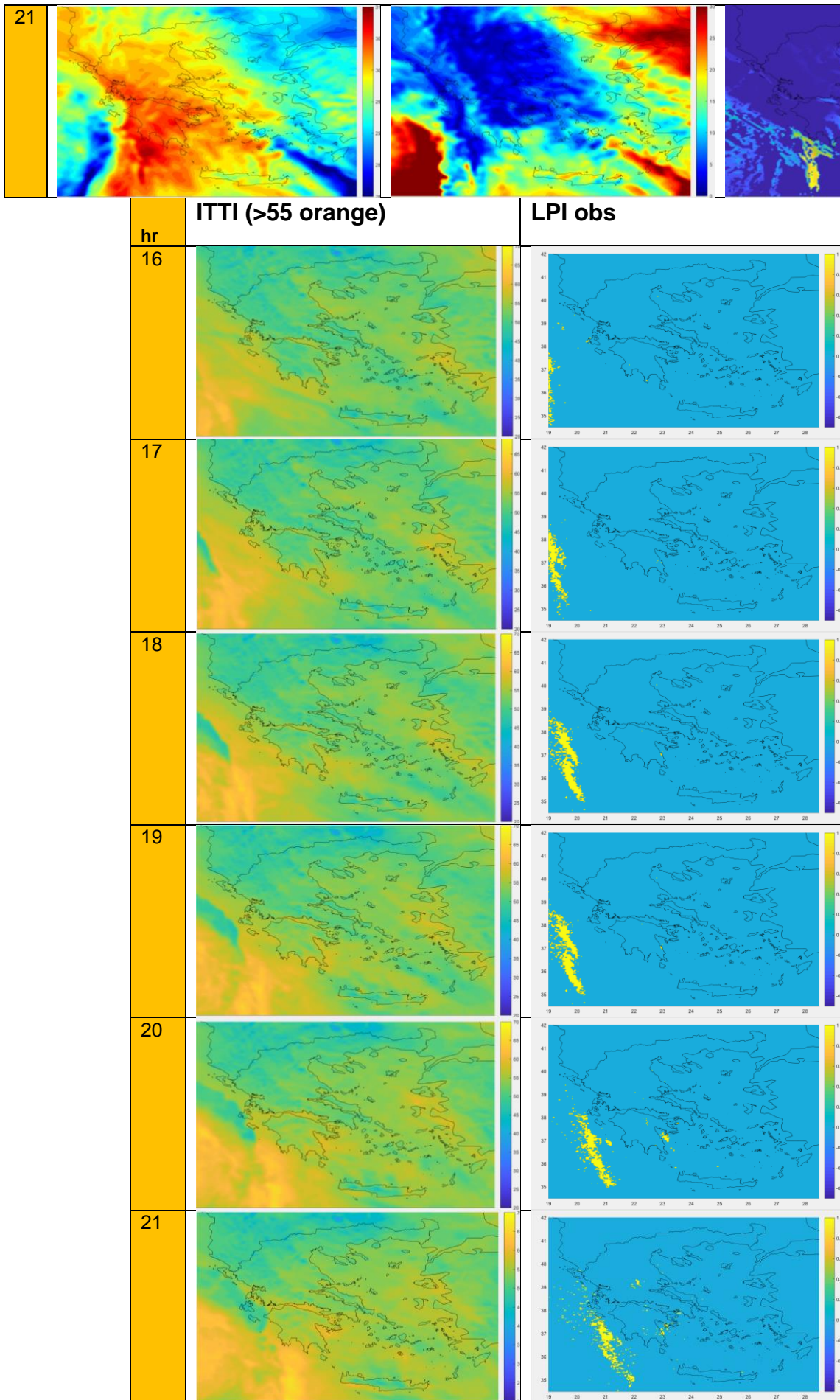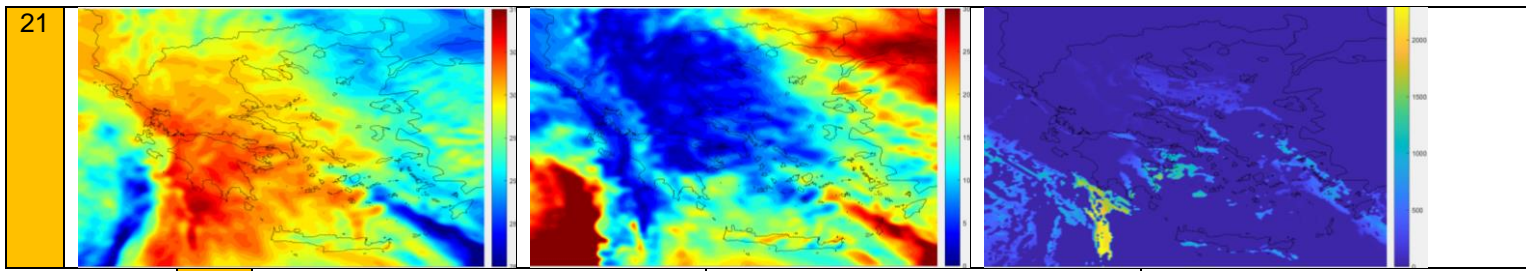

9. Recommendations

The main outcomes from the work performed for Task 3.5, can be summarized as follows:
- It is necessary to derive upscaled LPI products in resolution larger than 40km (10times the original one), in order to gain reliability in the forecasts. From the analyzed events, the performance of COSMOGR4 for LPI seemed to be strongly dependent on weather regimes.
- LPI raw values need to be thresholded according to the area and period examined. Further study for longer periods is necessary n order to determine what thresholds are appropriate for the specific geographic area.
- Thresholds for thermodynamical indices associated to severe thunderstorms need to be appropriately defined to provide useful indication of a thunderstorm area. Default values often do not apply.
- The lightning potential index produces reliable lightning information during stronger storms, much like observed in observational data. A general overestimation of the presence of lightning was derived when native resolution was used.
- 'Forecasters would be able to anticipate lightning activity from other model outputs such as CAPE or postprocessed thermodynamical indices even with less accuracy in the position, For forecasters the added value of direct LPI forecasts used proved to be very small, or not present at all.
- 'Probably, the LPI is somewhat better at distinguishing lightning-producing storms and this may be of importance to some user groups.

10.   References

Yair Y, Lynn B, Price C, Kotroni V, Lagouvardos K, Morin E, Mugnai A, Del Carmen Llasat M. Predicting the potential for lightning activity in Mediterranean storms based on the Weather Research and Forecasting (WRF) model dynamic and microphysical fields. Journal of Geophysical Research Atmospheres. 2010;115 :1–13.

Miller RC (1967) Notes on analysis and severe storm forecasting procedures of the Military Weather Warning Center: Tech. Report 200, AWS, USAF.

Johnson DL (1982). A stability analysis of AVE-4 severe weather soundings. NASA TP-2045 13: 8.

Grieser, J., 2012. Convection parameters. Selbstverl.

Saunders, C. P. R. (2008), Charge separation mechanisms in clouds, Space Sci. Rev., 137, 335– 353.

Moncrieff, M. W. and Miller, M. J. (1976): The dynamics and simulation of tropical cumulus and squall lines; Quart. J. Roy. Meteor. Soc., 102 373-394.